Accepted to J. Chem. Phys. 10.1063/5.0094367

Ab initio composite strategies and multireference approaches for lanthanide sulfides and selenides

Nuno M. S. Almeida[a], Timothé R. L. Melin[a], Sasha C. North[a], Bradley K. Welch[a], and Angela K. Wilson[a]*
[a]Michigan State University, Department of Chemistry, East Lansing, MI 48864, U.S.A
[*]akwilson@msu.edu

Abstract

The *f*-block *ab initio* correlation consistent composite approach (*f*-ccCA) was used to predict the dissociation energies of lanthanide sulfides and selenides. Geometry optimizations were carried out using density functional theory (DFT) and coupled cluster singles, doubles, and perturbative triples CCSD(T) with one-, and two-component Hamiltonians. For the two-component calculations relativistic effects were accounted for by utilizing a third-order Douglas-Kroll-Hess (DKH3) Hamiltonian. Spin-orbit coupling was addressed with the Breit-Pauli Hamiltonian within a multireference configuration interaction (MRCI) approach. The state averaged complete active space self-consistent field (CASSCF) wavefunctions obtained for the spin-orbit coupling energies were used to assign the ground states of diatomics, and several diagnostics were used to ascertain the multireference character of the molecules.

I. Introduction

Lanthanide compounds have a number of important uses such as in catalysis, phosphors and magnets, with applications in superconductors, hybrid cars, display devices, stealth technology, and potential anti-cancer agents.[1] Lanthanide chalcogenide (selenium and sulfur) clusters have been synthesized [2–4] for use in optical fibers [5–9] and lanthanide sulfides have applications in thermoelectric materials,[10] infrared window materials,[11] and photovoltaic energy materials.[12] In all of these applications, thermodynamic properties such as enthalpies of formation, bond dissociation energies, and reaction enthalpies, are of paramount important in understanding reactivity. However, fundamental properties such as such as bond dissociation energies (BDEs) can be difficult to describe for heavy element species.

Gaining structural and energetic insight about lanthanides requires both experiment and theory. Experimentally, there is a severe lack of small molecule experimental data. One of the reasons for the lack of experimental studies for some heavy element species is attributed to their radioactivity (for example promethium in the lanthanide series, and all the actinide series), limiting studies due to special facilities and/or requirements in their handling. Some elements are not naturally occurring, at least in appreciable amounts (promethium in the lanthanide series and all but uranium and thorium in the actinide series), and therefore must be synthesized, which can be a slow (sometimes an atom-at-a-time!) and costly process.

For lanthanide species, historically, the Knusden cell mass-spectrometry has been used to study equilibrium vapor properties at high temperature. Prior work, largely done from the late 1960's to the 1980's, has provided rare-earth gas phase thermodynamic data, including bond dissociation energies.[13–15] However, the bond dissociation energies determined from such experiments were obtained through the use of the second and third laws of thermodynamics, requiring high precision measurements, which were often not achieved with the Knusden cell approach. As well, the use of these laws required statistical thermodynamic assumptions, which led to significant errors for a number of species.[16]

Theory provides another route to address lanthanide species. However, due to the energetic complexity of lanthanide-containing molecules, *ab initio* calculations on these species can be computationally prohibitive (in terms of CPU times to obtain results, required memory and disk space) , so predictions for these species have traditionally been dominated by density functional theory (DFT). For example, Dolg *et. al.* performed DFT calculations using the B88 and P86 functionals combined with small core pseudopotentials (ECP) on lanthanide high spin complexes, specifically on GdX diatomics (X=H, N, O, F, P, S, Cl, Gd), to predict chemical binding. [17] Luo and coworkers used DFT approaches to predict the first ionization potentials for lanthanide monosulfides (LnS where Ln = La, Ce, Eu, Gd, Yb and Lu).[7] Three density functionals were used: the Becke functional for exchange correlation paired with Perdew (BP),[18] Perdew and Wang (BPW),[19,20] and Lee-Yang-Par (BLYP).[21] The Perdew functional yielded the smallest mean absolute deviations from the experimental first ionization potentials, and thus was employed to calculate bond lengths, vibrational frequencies, populations, and dissociation energies for the diatomic lanthanide sulfides. Xu *et. al*[22] examined the electronic configurations of LnX with Ln=La-Eu, and X=O, S, Se, and Te using relativistic DFT (VWN, PBE, BP, PW91 and BLYP functionals). The authors used the fractional occupation number approach to determine the ground state electronic configurations for the diatomic, concluding that a σ molecular orbital is involved in the bonding when the lanthanide atom has less than three electrons in its 4*f* orbital shell. The most intensive single reference-based computations to date were caried out on a set of lanthanum oxide and halides by Solomonik and Smirnov.[23] The authors utilized a coupled cluster based scheme that includes core-valence contributions and contributions from full triples, and perturbative quadruples, obtaining a mean absolute deviation (MAD) of 1.8 kcal mol^{-1}, showing the utility of the higher order coupled cluster contributions for a subset of the molecules (EuO, YbF, and LuO).[23]

Recent calculations utilizing the Ln54[24,25] and An66 sets,[26] sets of 54 lanthanide and 66 actinide enthalpies of formation and dissociation energies, with experimental uncertainties of 5 kcal mol^{-1} or less, have assessed the utility of a number of density functionals for heavy element species. For lanthanide molecules, the typical errors for these thermodynamic properties are on the order of 23 kcal mol^{-1}; the errors for the actinide molecules are on the order of 10 kcal mol^{-1}. The smaller errors for actinides are attributed to the more covalent bonding nature of actinide species, as compared to lanthanides. However, the errors in either case are not ideal. A leading reason for large errors in lanthanide and actinide chemistry pertains to the fact that available functionals have not been parameterized for use with the heavy elements. An additional drawback to the use of DFT is its difficulties in describing systems with degeneracies or near-degeneracies (multireference systems).[27] Even though approaches to multireference DFT have been developed, such as multiconfiguration pair-density functional theory (MC-PDFT), only recently have they begun to be considered for actinide complexes.[28] Most forms of DFT are less than ideal for the *f*-elements, as their partially filled valence shells often lead to multireference character. As well, as demonstrated in the Ln54 and An66 studies, the utility of the functionals deviates very substantially from molecule to molecule, depending upon lanthanide or actinide, ligand, and property, with differences that can be as large as 100 kcal mol^{-1} or more for the dissociation energy or enthalpy of formation, complicating the choice of functional. For example, the enthalpy of formation obtained for the UO_3 molecule in the An66 set is -243.8 kcal mol^{-1} when using the SVWN functional, and -141.3 kcal mol^{-1} when using the BHLYP functional.[26]

High quality experimental data with small experimental error bars has been vital to gauging the utility of theoretical methods in earlier parts of the periodic table. For the heavy elements, not only are the numbers of studies limited, even some of the very best results have had large experimental uncertainties. For example, for diatomic lanthanide sulfides and selenides in particular, there are few experimental studies[29–32] where the bond dissociation energies have been determined. The studies, which occurred in the 1960's and 1970's, resulted in errors of ~15 kJ mol^{-1} or 0.2 eV, which is near the value selected for "lanthanide chemical accuracy" (5 kcal mol^{-1}).[24] This term was proposed more recently, based upon the average experimental uncertainties in the determination of enthalpies of formation and bond energies for a set of 54 lanthanide energies, which were then utilized to gauge predictions by a number of density functional approaches.[24] Such large experimental uncertainties, though somewhat useful (as some data is better than none), make it more difficult to assess computational methodologies.

Recently, new experiments have enabled unprecedented accuracy in the prediction of dissociation, with an estimated accuracy of ~0.004 eV.[33] The Morse group has utilized a predissociation-based two-photon ionization (R2PI) method[34] to obtain bond dissociation energies for these species for transition metal and inner transition metal (*f*-element) containing silicides,[35–37] selenides, [38] and sulfides.[38] The R2PI method makes use of the spin-orbit and non-adiabatic couplings of the large density of electronic states near the ground separated atom limit that allow the molecules to predissociate rapidly when the bond dissociation energy is reached or exceeded. Predissociation in this case is molecular dissociation that occurs long before the separated atom limit is reached. It is the key phenomenon, that allows bond dissociation energies of transition metal and inner-transition metal molecules to be measured with high precision. When a predissociation threshold is observed by a sharp drop in signal in the absorption spectrum of the molecule of interest, its value directly provides the BDE of the system. The predissociation technique is a significant breakthrough in the determination accurate thermodynamic data.

When considering the often-prohibitive computational cost of *ab initio* electron correlation calculations on heavy element containing species, composite methods are uniquely suited to provide accurate results with respect to experimental energies and thermodynamic properties while lowering the computational cost compared to traditional *ab initio* methods. Among the most used composite methods are the Gaussian-*n* (G*n*),[39–44] Weizmann-*n* (W*n*), [45–48] Complete Basis Set (CBS-*n*),[49–54] High accuracy extrapolated *ab initio* thermochemistry (HEAT),[55–58] Feller-Peterson-Dixon (FPD),[59–61] and our own correlation consistent Composite Approach (ccCA).[62–64] ccCA was first constructed for use on main group species; for main group and s-block metals, ccCA was shown to achieve chemical accuracy (±1 kcal mol^{-1}), on average.[62–65] Later the method was developed for use with 3*d* transition metals (ccCA-TM)[66–68] achieving *transition metal chemical accuracy* (±3 kcal mol^{-1}), on average, for the prediction of over 200 transition metal enthalpies of formation. Recently, Welch *et. al.* introduced Super-ccCA (s-ccCA), a composite method capable of achieving transition metal dissociation energies of <1-2 kcal mol^{-1} within those from R2PI experiments. s-ccCA utilizes contributions to the composite including higher-level coupled cluster corrections (triple and quadruple excitations) and spin-orbit contribution/correction from a Breit-Pauli Hamiltonian.[69] The theoretical predictions were compared to experimental R2PI results.[35–37,70,71] Recently, *f*-ccCA has been applied to lanthanide complexes, namely oxides and halides, which were also compared to experimental R2PI predissociation energy results.[72,73]

A challenge, however, for single reference methodologies, is that they can fail for lanthanide chemistry, as a single reference determinant may not be able to describe low-lying excited states or may converge to the wrong ground state. As well, Hartree-Fock orbitals used as initial guess orbitals may not be able to properly describe the ground state and lead to erroneous convergence issues. [74,75] Paired with composite methods, multiconfigurational approaches are typically necessary for lanthanide complexes, to obtain accurate thermochemical and spectroscopic properties. The detailed work of Ruedenberg *et. al.* on the nature of the chemical bond, localized orbitals, and on Full Optimized Reaction Spaces (FORS), led to the widely used complete-active-space self-consistent-field (CASSCF)) approach and demonstrated the importance of multireference approaches.[76–79] By using multireference approaches, correct energetic assessment of ground states and spin-orbit contributions can be performed confidently, and will be considered in this effort.

Herein, *f*-ccCA has been used for the determination of bond dissociation energies of lanthanide sulfides and selenides. The highly accurate bond dissociation energies from Morse provide an excellent gauge of the ability of ccCA to model this molecular property for these lanthanide species.

II. Computational details

Geometry optimizations were performed for each of the molecules (Ln-S and Ln-Se (Ln = Pr, Nd, Sm, Eu, Gd, Tb, Er and Lu) using two different methods: the nonlocal exchange-correlation Perdew and Wang (PW91) functional[80] and coupled cluster with single, double, and perturbative triple excitations [CCSD(T)]. PW91 was selected for its demonstrated efficacy for transition metals in bond dissociation predictions and as guess orbitals, which are important to describe the ground state correctly and for obtaining accurate thermodynamic properties.[81] Even though, Hartree-Fock orbitals are used throughout *f*-ccCA, if there are significant differences between these orbitals and natural orbitals, the calculation of accurate thermodynamic properties can be difficult.[74,82] For example, for the NdS complex studied herein, the ground state is composed of a linear combination of four determinants. CCSD(T) was utilized due to its overall utility in predicting bond dissociation. Two routes were utilized to incorporate relativistic effects.

The first was the use of a third-order Douglas-Kroll-Hess Hamiltonian (DKH3) which was considered for PW91 and CCSD(T) and will be referred to PW91-DKH3 and CCSD(T)-DKH3, respectively throughout the discussion.[83] For these calculations, the cc-pVTZ-DK3[84] basis set for lanthanides, aug-cc-pV(T+d)Z-DK[85,86] for sulfur, and aug-cc-pVTZ-DK[87] for selenium were utilized. The other route was to use effective core potentials (ECP) which will be referred to CCSD(T)/ECP. For each lanthanide, an atomic natural orbital (ANO) basis set was used with the corresponding ECP28MWB[88–90] pseudopotential, accounting for scalar relativistic effects. For sulfur and selenium, aug-cc-PV(T+*d*)Z and aug-cc-pVTZ-PP with a ten electron ECP (ECP10MDF) were employed, respectively.[91]

A triple-ξ level basis set was utilized for the geometry optimization steps, due to its utility with respect to experiment and computational cost.[92] In prior work on LuF, for example, despite the significant gain in computational cost incurred by the use of a quadruple-ξ level basis set, the bond length did not improve, and even the triple-ξ level basis set led to a CCSD(T) optimized structure that was within 0.002 Å of experiment.[92] In the present work, frequencies were calculated to correct for zero-point energies (ZPEs), which were also determined at the triple-ξ level. For the CCSD(T) geometry optimizations, restricted Hartree-Fock (RHF) orbitals were generated and then used as guess orbitals for unrestricted CCSD(T) calculation (for the open-shell systems) and restricted CCSD(T) (closed-shell systems). The calculations were performed with MOLPRO 2020.[93] In MOLPRO 2020, the abelian point group, C_{2v} was utilized, as the full point group symmetry (C_∞) is not available for diatomics.

In the second part of this work, the *f*-ccCA *ab initio* composite scheme, recently introduced by Welch *et. al*, was used to obtain the dissociation energy (D_0) for each of the lanthanide compounds.[73] The *f*-ccCA dissociation energy was obtained using Equation 1:

$$E(f-ccCA) = E_0(f-ccCA) + \Delta E(CC) + \Delta \mathrm{E(CV)} + \Delta \mathrm{ZPE} + \Delta \mathrm{E(SO)} \tag{1}$$

where E_0(*f*-ccCA) corresponds to the reference energy, $\Delta E(CC)$ is the correlation contribution, $\Delta \mathrm{E(CV)}$ is the core-valence and core-core contribution, ΔZPE is the zero-point vibrational energy, and $\Delta \mathrm{E(SO)}$ is the spin-orbit coupling contribution. The reference energy, E_0(*f*-ccCA), is composed of the addition of two contributions: the Hartree-Fock (HF) energy and the Møller-Plesset second-order perturbation theory (MP2) correlation energy, each extrapolated to the complete basis set (CBS) limit. The HF reference energy (ΔHF_{CBS}) is obtained at the complete basis set limit using a two-points extrapolation scheme which was previously shown to be effective for composite schemes [94,95]:

$$E(n) = E_{CBS} + A\exp(-1.63n) \tag{2}$$

Using HF energies determined at the triple and quadruple-ζ basis set levels (cc-pVnZ-DK3, aug-cc-pV(n+d)Z-DK and aug-cc-pV(n)Z-DK for Ln, S and Se, respectively). In Equation 2, n represents the basis set level, E(n) represents the energy at the n^{th} basis set level, E(CBS) is the CBS limit and A, a coefficient. The MP2 reference energy ($\Delta MP2_{CBS}$) is calculated using the following three-point extrapolation scheme by Peterson *et al.*[96]:

$$E(n) = E_{CBS} + A\exp[-(n-1)] + B\ exp\ [-(-n-1)^2] \tag{3}$$

using energies determined at the double-, triple-, and quadruple-ζ basis set levels, using the same basis set as for the HF references. In Equation 3, A and B are two variables determined during the fitting of the energies. To account for correlation beyond the MP2 approximation, unrestricted coupled cluster single, double, and perturbative corrected triple excitations (UCCSD(T)) level calculations were performed at a triple-ζ level (ΔE(CC), see Equation 4):

$$\Delta E(CC) = E[UCCSD(T)/\text{cc-pVTZ-DK}] - \text{E[MP2/cc-pVTZ-DK]} \tag{4}$$

The core-valence and core-core contribution (ΔE(CV)) was determined employing UCCSD(T) and the cc-pwCVDZ[84] basis set with and without core the electrons:

$$\Delta E(CV) = E[UCCSD(T,FC1)/\text{cc-pwCVDZ-DK}] - \text{E[UCCSD(T)/cc-pwCVDZ-DK]} \tag{5}$$

where FC1 (frozen-core 1) corresponds to the calculation in which sub-valence electrons were included in the correlation space. For Pr, Nd, Sm, Eu, Tb and Er, the electrons included in the valence correspond to: $5s^2$, $5p^6$, $6s^2$, $4f^n$ (where n is the number of electrons). For Gd and Lu, the $5d^n$ electrons are also included in the correlation space. The $3s^2$ and $3p^4$ sulfur sub-valence and $4s^2$, $4p^4$, and $3d^{10}$ selenium sub-valence electrons are included in the correlation space. For the FC1 calculations, the following electrons are included in the correlation space: $4s^2$, $4p^6$, and $4d^{10}$ for lanthanides; $2s^2$ and $2p^6$ for sulfur, and $3s^2$ and $3p^6$ for selenium. The ΔZPE correction was obtained from the frequency calculation at the optimized geometry. The spin-orbit coupling (ΔE(SO)) is calculated using the following equation:

$$\Delta \mathrm{E(SO)} \;=\; \mathrm{SO(LnX)} - \sum_i SO(X_i) \tag{6}$$

where SO(LnX) is the spin-orbit correction for the molecule and SO(X_i) is the spin-orbit correction for each atom. For atomic spin-orbit (SO(X_i)), the corresponding spin-orbit energies of each ground state were obtained from the NIST database[97] and are *J* averaged. The atomic spin-orbit correction is determined using Equation 7:

$$SO(X_i) \;= \frac{\sum_J (2J\;+1)\Delta E_J}{\sum_J (2J+1)} \tag{7}$$

where J is the total angular momentum of the state and ΔE_J is the energy difference between the ground state and state J energies. For the molecular spin-orbit correction term SO(LnX)) a multireference wavefunction (using the complete active space self-consistent field (CASSCF) method) was constructed for Ln-S and Ln-Se complexes with a mixture of ground and close-lying excited states to obtain spin-orbit corrections for the ground state.

For the multireference wavefunction calculations, the $4f$ (f_{yz^2}, f_{xyz}, $f_{y(3x^2-y^2)}$, f_{xz^2}, $f_{z(x^2-y^2)}$, $f_{x(x^2-3y^2)}$, f_{z^3}) and $6s$ hybrid orbitals of the metal were included in the CASSCF active space, except for gadolinium and lutetium. For the former, the $5d$ ($d_{x^2-y^2}$, d_{z^2}, d_{xy}, d_{xz}, d_{yz}) hybrid orbitals were included in conjunction with the $4f$ and $6s$ orbitals. For lutetium, only the $5d$ and $6s$ hybrid orbitals were included in the active space, because the $4f$ set of hybrid orbitals are occupied by 14 electrons and thus do not have a large contribution towards spin-orbit coupling. The $3p_{x,y,z}$ and $4p_{x,y,z}$ set of orbitals from sulfur and selenium are doubly occupied at the equilibrium bond length and were not included in the CASSCF active space. For MRCI, the same active space that was utilized for the CASSCF calculations was chosen. In addition, the $3p$ and $4p$ orbitals for sulfur and selenium, respectively, were also considered. The inclusion of these p orbitals allows for single and double excitations from these orbitals to the active space in the MRCI calculations (orbitals were included at the "core" level in the MOLPRO implementation).[93] The spin-orbit coupling energies were calculated using the Breit-Pauli Hamiltonian and the MRCI wavefunction. The ground and first excited states were included in the state-averaged CASSCF calculations. Then, the CI vectors and energetics for MRCI were utilized to gauge potential multireference character in the diatomic by comparing the weight of configurations. As well, for all of the molecules, the multireference character was assessed by determining the T_1 and D_1 diagnostics[98,99], coupled cluster singles and doubles amplitudes ($|T_{1max}|$ and $|T_{2max}|$, respectively)[100], and spin contamination at the triple-ζ level.

For several species (TbS, TbSe, ErS and ErSe), CCSD(T)-DKH3 energies were determined at the double-, triple- and quadruple-ξ basis set levels (as described following Equation 3) and were extrapolated to the CBS limit using Equation 3. Two different guess orbitals (RHF and RPW91) were utilized for CCSD(T).

For ErSe, a functional from each of four density functional families - local-density approximation (LDA), generalized gradient approximation (GGA), meta-GGA(M-GGA) and hybrid M-GGA) - was employed for bond dissociation energy predictions. The corresponding functionals were PW91 (LDA), Tao, Perdew, Staroverov, Scuseria (TPSS, GGA),[101] Minnesota 2006 local functional (M06-L, M-GGA)[102] and the Becke, 3-parameter, Lee -Yang -Parr (B3LYP, hybrid M-GGA)[18,103] were utilized at a restricted level (RKS). These DFT calculations were performed at a triple-ξ level as already described.

II. Results and discussion of results

A. Geometry optimization of sulfides and selenides

In Table I, the optimized bond lengths and vibrational frequencies determined for the PW91 and CCSD(T) calculations for the sulfide complexes (Pr, Nd, Sm, Eu, Gd, Tb, Er and Lu) are provided. In terms of bond lengths, though a contraction in bond length is expected while the *f* shell is being filled, due to the complexity of the electronic structure of lanthanide chemistry, this was not observed for the sulfide diatomics.[22] In Table I, CCSD(T) bond lengths for both one- and two-component Hamiltonians are longer for PrS to GdS, and LuS than for the corresponding PW91 optimized structures. The difference in bond length for lanthanide sulfides comparing PW91 and CCSD(T) ranges from ~0.01 Å (GdS and LuS) to ~0.05 Å for EuS. NdS has a 0.02-0.03Å shorter bond length than the DFT(ZORA) at triple-ζ bond length given by Xu *et. al.*[22] This difference is not surprising, as NdS has significant multireference character, requiring four CI vectors to describe the ground state (Table VII). For RHF and CCSD(T), the lowest electronic configuration corresponds to having unpaired electrons in the $4f_{z^3}$, $4f_{z(x^2-y^2)}$, and 6*s* orbitals and another unpaired electron in the $4f_{x(x^2-3y^2)}$ or $4f_{y(3x^2-y^2)}$ orbital (Table VII). Even though this configuration is an excited state at the CAS/MRCI level, it is the ground state electronic structure for RHF and UCCSD(T).

For ErS and TbS complexes, their bond lengths are larger with PW91 than with CCSD(T). The vibrational frequencies for CCSD(T) with a two-component Hamiltonian are 60.44 and 83.31 cm^{-1} larger than the PW91-DKH3 frequencies for TbS and ErS, respectively. For the CCSD(T) calculations with a one-component Hamiltonian and an ECP basis set, there was no convergence for the SCF procedure for TbS and ErS (which is discussed in the next section).

Overall, the difference in the bond length from one- and two-component Hamiltonian predictions was not very significant; on average, CCSD(T)-DKH3 bond lengths are ~0.01 Å longer than for CCSD(T)/ECP for all complexes. The results herein are on par with DFT, SCF and CISD bond lengths predicted in prior studies, and shown in Table I. However, in comparing theoretical and experimental bond lengths, there are some substantial differences. For example, for EuS and GdS the differences between CCSD(T)-DKH3 and experiment are large, ~0.08 Å for EuS and ~0.16 or 0.08 Å for GdS, depending upon experiment used for comparison. The substantial difference in bond length can be attributed to the estimated experimental bond lengths, rather than having direct measurements. For lanthanide sulfides, a one component Hamiltonian CCSD(T), with a robust ECP basis set can recover most of the electron correlation needed.

In Table 2, the optimized geometry for the selenide complexes (Pr, Nd, Sm, Eu, Gd, Tb, Er and Lu) are provided. For the one-component Hamiltonian predictions, selenide complexes have ten more electrons than the sulfides, which were treated with an ECP. The shorter bond distances obtained in the calculations relative to experiment for sulfide complexes also occurs for selenides, but it is not as pronounced. The difference in bond lengths between PW91 and CCSD(T) is quite large for SmSe, the difference is ~0.14 and ~0.15 Å, for one- and two-component Hamiltonian predictions respectively. For the other seven selenium complexes, the bond lengths differ on average by ~0.01 Å between PW91 to CCSD(T), except for EuSe, which is 0.04 Å. NdSe has a shorter bond length than the FON-DFT results using the ZORA Hamiltonian (0.04-0.05Å). The four different CI vectors needed to describe the ground state determinant make NdSe a multireference system (see Table VII), akin to NdS. For TbSe and ErSe, as for TbS and ErS, the bond length is larger for PW91 than for CCSD(T), and also, the ground state vibrational frequencies are smaller for PW91. In addition, the CCSD(T)/ECP optimization was also not possible due to the non-convergence of the SCF procedures. Overall, the equilibrium geometries are quite similar when comparing DFT (PW91) to CCSD(T). Comparing the CCSD(T) one- and two-component Hamiltonian bond length predictions, the difference is quite small, less than 0.01 Å for most complexes, and their vibrational frequencies differ by a maximum of ~5 cm^{-1}. The impact on the BDE predictions among the different geometries for all complexes is always less than 0.8 kcal mol^{-1}.

Table I. DFT (PW91-DKH3), CCSD(T)/ECP and CCSD(T)-DKH3 optimized bond lengths (Å) and harmonic vibrational frequencies (cm^{-1}) (in parenthesis) of sulfide complexes using a triple-ζ level basis set.

Molecules	PW91-DKH3	CCSD(T)/ECP	CCSD(T)-DKH3	Previous theoretical predictions	Exp.
PrS	2.3154 (450.81)	2.3291 (459.21)	2.3310 (455.43)	2.347[22,a] (432.7)[22,a] 2.338[22,b]	-
NdS	2.3258 (428.93)	2.3251 (459.44)	2.3289 (456.73)	2.345[22,a] (447.5)[22,a] 2.340[22,b]	-
SmS	2.4186 (393.14)	2.4388 (375.16)	2.4378 (380.34)	2.414[22,a] (390.6) 2.334[22,b]	-
EuS	2.3879 (384.25)	2.4315 (376.50)	2.4373 (374.56)	2.41[7,e] (362[7,e]) 2.396[22,a] (383.5)[22,a] 2.343[22,b]	2.51[106,c] (400)[106,d]
GdS	2.2945 (436.62)	2.3019 (457.65)	2.3119 (453.89)	2.31, 2.29[7,e] (431[7,e]) 2.272-2.342[17,f] (412-493)[17,f]	2.15[106,c] 2.23 [106,c] (479) [106,c]
TbS	2.3309 (398.22)	-	2.3033 (458.66)	-	-
ErS	2.3329 (372.70)	-	2.2834 (456.01)	-	-
LuS	2.2572	2.2611	2.2762	2.27[7,e]	2.17[106,c]

	(448.17)	(452.87)	(447.03)	(456[7,e])	2.10[106,c] (500)[106,c]

[a] FON-DFT calculation using ZORA Hamiltonian at a tiple-ζ level. [b] FON-DFT calculation using Spin-orbit coupled calculations [c] Estimated from empirical relations. [d] Estimated based on experiments. [e] DFT calculations using the BP, BPW and BLYP functional at the triple-ζ level. [f]All electron DFT (LDASIC, B88 and B88P86) calculations and ECP calculation with SCF, CISD and ACPF at the ANO triple-ζ level.

Table II. DFT (PW91), CCSD(T) with and ECP and CCSD(T)-DKH optimized bond lengths (Å) and harmonic vibrational frequencies (cm^{-1}) (in parenthesis) of selenium complexes using a triple-ζ level basis set.

Molecules	PW91/DKH3	CCSD(T)/ECP	CCSD(T)/DKH3	Previous theoretical predictions[22,a]
PrSe	2.4610 (300.15)	2.4730 (308.40)	2.4781 (305.67)	2.504 (284.8) 2.497
NdSe	2.4745 (282.50)	2.4669 (307.38)	2.4738 (306.60)	2.519 (255.6) 2.523
SmSe	2.4347 (259.35)	2.5761 (252.27)	2.5831 (253.10)	2.508
EuSe	2.5325 (252.01)	2.5457 (248.01)	2.5804 (248.27)	2.552 (250.9) 2.502
GdSe	2.4236 (287.53)	2.4390 (302.68)	2.4514 (300.44)	-
TbSe	2.4526 (263.78)	-	2.4426 (301.41)	-
ErSe	2.4852 (238.22)	-	2.4182 (295.43)	-
LuSe	2.3913 (288.66)	2.3901 (292.76)	2.4059 (290.31)	-

[a] FON-DFT calculation using ZORA Hamiltonian at a tiple-ζ level.

B. Bond dissociation energies for lanthanide sulfides and selenides

In this section, using the three different geometries described above, *f*-ccCA is employed to calculate BDEs for eight sulfide and selenide complexes, and the BDEs are compared to experiment. The molecules are separated into three categories, depending upon the error in the *f*-ccCA dissociation energy predictions relative to Morse's experimental data (see ref[38]): Cat I (± 2 kcal mol^{-1}), Cat II (± 6 kcal mol^{-1}) and Cat III (> 6 kcal mol^{-1}). These differences are presented in Figure 1. In Table III, a summary of the *f*-ccCA dissociation energies determined at each different optimized geometry is provided and compared with experiment. Moreover, in Tables IV, S1 and S2, the total atomization terms and dissociation energy predictions for CCSD(T)-DKH3, PW91-DKH3 and CCSD(T)/ECP geometries are shown.

The calculated dissociation energies (D_0) for sulfide and selenide complexes are decomposed into the different contributions that comprise the *f*-ccCA composite, as described in the methodology section.

The reference energy (ΔMP2$_{\mathrm{CBS}}$ and ΔHF$_{\mathrm{CBS}}$), core-valence (ΔCV), correlation contribution (ΔCC), and spin-orbit (ΔSO) contributions. Table V provides TbS, ErS, TbSe and ErSe bond dissociation energies calculated with two different approaches: RHF and DFT (PW91) orbitals. In Table VI, dissociation energies considering different families of DFT are used to predict the most problematic lanthanide complex: ErSe. Table VII contains the corresponding CI vectors for the spin-orbit correction for each of the sulfide and selenide complexes. In Table VIII, multireference diagnostic are given for all sulfide and selenide complexes at CCSD(T)-DKH3 geometries. For PW91-DKH3 and CCSD(T)/ECP geometries, see Tables S3 and S4 in the supporting information for the corresponding diagnostics.

For the sulfide complexes, *f*-ccCA was quite successful for PrS, SmS, GdS and LuS, resulting in differences of 1-2 kcal mol^{-1} from experiment for each of the three investigated geometries (PW91-DKH3, CCSD(T)/ECP and CCSD(T)-DKH3). These four complexes are part of Cat I. The ground state of these four complexes has been identified as: PrS (^{4}H), SmS ($^7\Delta$), GdS ($^9\Sigma^-$) and LuS ($^2\Sigma^+$). The ΔMP2$_{\mathrm{CBS}}$ term for these four complexes ranges between 37 and 51 kcal mol^{-1} and the core-valence term (CV) contributes 1-2 kcal mol^{-1} to the total energy. The correlation term (CC) ranges from -4.75 (SmS) to 6.48 (PrS) considering CCSD(T)-DKH3 geometries (Table IV). The spin-orbit correction obtained with the Breit-Pauli Hamiltonian can render a large difference in the final BDEs, with contributions that can be as large as -3.91 kcal mol^{-1}, as for LuS. Even though the molecule has small spin-orbit coupling, the individual atoms account for this large contribution. The choice of method for geometry optimization (PW91-DKH3, CCSD(T)-DKH3 and CCSD(T)/ECP) has very little impact on the energy, each resulting in a BDE for LuS within ~ 0.01 kcal mol^{-1} from experiment (Table III).

For NdS (^{5}I) (Cat II), the BDE is ~5 kcal mol^{-1} from experiment when the different optimized geometries are considered (shown in Tables IV, S1 and S2). When investigating the ground state of the neodymium atom (Nd), the electronic structure is more complex, which is a hurdle while treating these molecules with single reference methods. The neodymium ground state is a ^{5}I, resulting in 11 ways of constructing the ground state.[97] However, at the Hartree-Fock level, all electronic configurations are not all balanced in the same way; they are not all degenerate. For neodymium, the lowest energy at Hartree-Fock was obtained by placing two unpaired electrons in the same symmetry, and the other two in two different symmetries. In addition, in Table VII, for NdS there are four equally important CI coefficients (0.50), resulting in a complex ground state. In Table VIII, the D$_1$ value is 0.10 and the $|T_{1\mathrm{max}}|$ for this complex is 0.13, which is one of the highest among the studied complexes. The reference value for D$_1$ and $|T_{1\mathrm{max}}|$ for transition metals is 0.15 and 0.05 respectively.[104] The multireference ground state of NdS, i.e, for large CI contributions (see Table VII), along with a bad set of guess orbitals for the complex led to predictions that are ~ 5 kcal mol^{-1} from experiment.

For EuS ($^8\Sigma^-$) (Cat II), the spin-orbit contribution from the ground state of the complex is large (4.44 kcal mol^{-1} at the CCSD(T)-DKH3 geometry), though, for europium and sulfur atoms the spin-obit splitting is zero, and close to zero, respectively. The largest CI coefficient for EuS is 0.99 (Table VII), and its ground state is a $^8\Sigma^-$; here, a difference of 5 kcal mol^{-1} from experiment in the BDE was obtained. At the CAS/MRCI level, a $4f^6\,6s^1$ electronic configuration is predicted (see Table VII); while at RHF/UCCSD(T), a $4f^7 6s^0$ configuration is obtained. Single reference methods cannot predict the correct configuration for the ground state, which leads to a larger difference when compared to experiment. Similarly, for SmS, CASSCF predicts a ground state that has one electron in the 6*s* orbital ($4f^5 6s^1$), rather than in a $4f^6$ configuration. In addition, at HF/CCSD(T) the ground state converges to a $4f^6$ electronic configuration. However, for SmS, the impact of electron configuration in the final predicted BDE was small when compared to experiment.

The last two molecules TbS ($^8\Phi$) and ErS ($^5\Delta$) which are part of Cat III, are the most problematic complexes to treat with single reference methodologies. TbS primarily has one large contribution to the ground state, but the Tb (^{6}H) atom is quite multireference in nature. ErS has five main CI contributions to the ground state (see Table VII), which make it quite complex to address using single reference methods. In addition, in Table I, these two complexes have two of the largest $|T_{1max}|$ amplitudes, which can generate issues for Hartree-Fock initial orbital guesses resulting from multireference character. For TbS and ErS, the $\Delta MP2_{CBS}$ term is negative (-30.65 and -68.77 kcal mol^{-1} for PW91-DKH3 and -29.85 and -67.29 kcal mol^{-1} for CCSD(T)-DKH3, respectively), which means that according to MP2, the molecular complexes do not form, i.e, the atoms are more stable than the complexes. The coupled cluster correction, along with HF/CBS extrapolation make up for the negative MP2 energetics, and the final *f*-ccCA values are ~10 and 9 kcal mol^{-1} from experimental energies for TbS and ErS, respectively. Since the *f*-ccCA procedure is not very accurate for these complexes likely due to their multireference nature, other approaches to predict bond dissociation energies were taken.

In Table V, the CCSD(T)/CBS energies obtained at the CCSD(T)-DKH3 and PW91-DKH3 geometries are provided. For TbS, UCCSD(T)/CBS resulted in BDEs that are further from experiment than the *f*-ccCA BDEs. For example, UCCSD(T)/CBS using CCSD(T)-DK3 geometry renders a BDE of 137.0 kcal mol^{-1}, *f*-ccCA with the same geometry renders a BDE of 132.87 kcal mol^{-1}, and the experimental BDE is 122.0 kcal mol^{-1}. However, for ErS, the BDE was ~6 kcal mol^{-1} from experiment. Since Hartree-Fock provides a bad initial guess for these complexes, DFT orbitals were considered for CCSD(T), probing their effect on dissociation energy predictions. For TbS, DFT orbitals are a better guess for the complex, however they are not for ErS. Our best estimate for TbS is 4 kcal mol^{-1} from experiment using PW91 orbitals, but for ErS, CCSD(T) using RHF orbitals provides the most accurate result (92.5 kcal mol^{-1} obtained using UCCSD(T)/CBS vs 98.2 kcal mol^{-1} from experiment).

The lanthanide selenides also proved to be challenging for single reference wavefunction-based methodologies. As seen for the sulfide complexes, the Cat I molecules: PrSe (^{4}H), SmSe ($^7\Delta$), GdSe ($^9\Sigma^+$) and LuSe ($^2\Sigma^+$) resulted in bond dissociation energies within 1-2 kcal mol^{-1} when compared to the experimental values determined by Sorensen *et. al.*.[38] Furthermore, PrSe has the largest $|T_{2max}|$ in Table VIII which is within the threshold of multi-reference complexes ($|T_{2max}| > 0.15$).[104] However, the predicted dissociation energies are still accurate compared to experiment when calculated using single reference methodologies. In Tables S1 and IV the BDEs for PrSe obtained using the PW91-DKH3 and CCSD(T)/DKH3 geometries and the *f*-ccCA composite method are 102.35 and 102.24 kcal mol^{-1}, respectively, compared to the experimentally determined BDE of 103.68 kcal mol^{-1}. Regarding the other complexes of Cat I: GdSe and LuSe are indicated to be of single reference character based upon the diagnostics in Table VIII. In addition, they only have one main CI coefficient (see Table VII), so are expected to perform better with single reference methodologies.

NdSe (Cat II), which has ^{5}I ground state and has the same four CI coefficients as NdS, has a ground state with significant multireference character. It also has a large $|T_{1max}|$ value of 0.13 and D_1 of 0.10 (Table VIII). Due to the complexity of the electronic structure of this complex and the mixing of states, the spin-orbit contribution of this complex is quite large (-3.84 kcal mol^{-1} at the CCSD(T)-DKH3 geometry). The dissociation energies determined at each of the optimized geometries, are ~5 kcal mol^{-1} from experiment.[38] For EuSe ($^8\Sigma^-$) (Cat II), similar observations to those made for EuS are made for the BDE and spin-orbit contribution: the BDE is ~6 kcal mol^{-1} from experiment, with a large spin-orbit contribution of 2.77 kcal mol^{-1}. Its ground state also converges to a $4f^7$ configuration as was seen for EuS, while at the CAS/MRCI level a $4f^66s^1$ electronic configuration is observed. For SmSe, the $4f^56s^1$ configuration is also more stable with a multireference wavefunction (CASSCF) than a $4f^6$ configuration.

Focusing on the Cat III compounds: TbSe and ErSe, the same observations made for TbS and ErS are again seen here. The ΔMP2$_{\mathrm{CBS}}$ term is negative for both complexes. For ErSe values of -181.13 and -183.70 kcal mol^{-1} are obtained for the PW91-DKH3 and CCSD(T)-DKH3 optimized structures, respectively. For TbSe a less negative term is observed (~-35 kcal mol^{-1} for both PW91-DKH3 and CCSD(T)-DKH3), but according to MP2 the atoms are more stable than the complex. For ErSe, not only does MP2 fail for this complex, but in contrast to what happens for the sulfides, this large difference is not corrected by the CCSD(T) calculation (correlation term) with the composite, so large negative values for the dissociation energy are obtained at *f*-ccCA level. For TbSe, ΔHF$_{\mathrm{CBS}}$ and ΔCC terms show that the complex forms, but it is due to error cancellations. On the contrary to their sulfide counterpart, for ErSe, the ΔHF$_{\mathrm{CBS}}$ and ΔCC terms are not enough to compensate for the huge negative ΔMP2$_{\mathrm{CBS}}$ term, leading to the negative dissociation energies, which means at *f*-ccCA level, ErSe does not form. The largest $|T_{1\mathrm{max}}|$ and D_1 for this complex are 0.25 and 0.18, which correspond to the largest values for these diagnostics found in Table VIII. In Table V, CCSD(T)/CBS energies are given. The dissociation energy predictions (obtained using the PW91-DKH3 and CCSD(T)-DHK3 geometries) for TbSe and ErSe are quite far away from experiment and, for ErSe the complex does not form according to CCSD(T)/CBS. It is clear from this table how poor the restricted Hartree-Fock guess orbitals are for these complexes. In Table V, for TbSe and ErSe DFT orbitals are also used as guesses for CCSD(T). For TbSe, these sets of orbitals prove to be of value and are better guesses for CCSD(T), which put the dissociation energy extrapolated at CCSD(T)/CBS at 4 kcal mol^{-1} from experiment. However, for ErSe, even with DFT orbitals the dissociation energy is still negative. The use of a multireference wavefunction could help in determining the bond dissociation energy. The ground state of Er is a ^{3}H, which leads to a large number of states generated and can complicate the determination of the complete dissociation channel (Er (^{3}H) + S (^{3}P)). In addition, even MRCI+Q is not a size extensive method, which carries an additional layer of complexity to these calculations. Since ErSe is such a difficult complex from an electronic structure perspective, DFT was probed and different functionals were considered for calculating dissociation energies for ErSe. DFT offers a computationally less costly theoretical approach than *ab initio* correlated methods that can lead to an easy comparison to experimental values. In Table VI, four families of DFT were considered using one representing functional from each family, and three different levels of basis sets. The meta-GGA functional, M06-L, obtained the closest results to experiment at a quadruple-ζ level. However, fortuitous error cancelation is the most likely cause for these predictions, because when comparing double- and triple-ζ results a consistent trend is not present. TPSS and PW91 completely fail predicting the dissociation energies. Finally, for the hybrid functional, B3LYP, there is a sudden drop in dissociation energy from the triple-ξ to quadruple-ξ levels. As demonstrated in ref [25] the performance of different density functionals for lanthanide containing species can be erratic at best, and this can be magnified with increasing or decreasing basis set size.[30] The DFT predictions are "disturbingly remarkable" and are surely the “right answer for the wrong reason”.[105]

Figure 1: *f*-ccCA BDE divided in three categories based on their difference from experiment[a,38]: Cat I (± 2 kcal mol^{-1}), Cat II (± 6 kcal mol^{-1}) and Cat III (more than 6 kcal mol^{-1})

Accepted to J. Chem. Phys. 10.1063/5.0094367

Table III: *f*-ccCA dissociation energy for each geometry optimization method and corresponding experimental data in kcal mol^{-1}.

Molecules	**PW91/DKH3**	**CCSD(T)/ECP**	**CCSD(T)/DKH3**	$Exp\ D_0$[38]	$Exp\ D_0$
Category I					
PrS	118.69	118.59	118.57	120.61	112 ± 6[a]
PrSe	102.35	102.29	102.24	103.68	-
SmS	92.70	92.63	92.65	92.52	-
SmSe	78.66	81.41	81.38	80.62	-
GdS	121.06	121.04	120.95	121.80	124 ± 6[a] 125 ± 4[b]
GdSe	105.77	105.74	105.63	106.20	102 ± 5[a] 103 ± 4[c]
LuS	119.69	119.62	119.62	119.70	120 ± 6[a] 120 ± 4[b]
LuSe	106.51	106.51	106.39	106.10	99 ± 6[a] 100 ± 4[c]
Category II					
NdS	116.73	116.53	116.50	111.15	120 ± 6[a] 112 ± 4[b]
NdSe	99.21	99.28	99.35	94.53	91 ± 6[a] 91 ± 4[c]
EuS	92.35	92.43	92.42	87.90	86 ± 6[a] 86 ± 4[b]
EuSe	82.34	82.40	82.32	76.50	66 ± 6[a] 72 ± 4[c]
Category III					
TbS	132.13	-	132.87	122.00	-
TbSe	92.02	-	92.47	106.10	-
ErS	89.01	-	89.94	98.20	99 ± 4[b]
ErSe	-100.29	-	-100.92	82.70	-

[a]Ref 13 [b]Ref 30 [c] Ref 31

Table IV. Total atomization terms and dissociation energy obtained with *f*-ccCA using CCSD(T)-DKH3 geometries, along with all electron basis sets. Theoretical and experimental dissociation energies are in kcal mol^{-1}.

	$\Delta MP2_{CBS}$	ΔHF_{CBS}	ΔCV	ΔCC	$\Delta\ SO$	$f-ccCA\ D_0$	$Exp\ D_0$[38]	$Exp\ D_0$
Category I								
PrS	44.69	69.70	1.65	6.48	-2.66	118.57	120.61	112 ± 6[a]
PrSe	39.44	56.99	2.66	8.83	-4.82	102.24	103.68	-
SmS	50.36	47.06	-0.64	-4.75	1.17	92.65	92.52	-
SmSe	43.52	41.31	0.62	-2.39	-1.32	81.38	80.62	-
GdS	48.71	79.69	0.61	-4.33	-3.08	120.95	121.80	124 ± 6[a] 125 ± 4[b]
GdSe	43.53	68.33	1.49	-2.06	-5.22	105.63	106.20	102 ± 5[a] 103 ± 4[c]
LuS	37.74	88.45	1.22	-3.22	-3.91	119.62	119.70	120 ± 6[a] 120 ± 4[b]
LuSe	36.45	77.54	0.63	-1.69	-6.12	106.39	106.10	99 ± 6[a] 100 ± 4[c]
Category II								
NdS	29.26	88.39	1.77	-1.47	-0.22	116.50	111.15	120 ± 6[a] 112 ± 4[b]
NdSe	24.10	76.28	2.83	0.72	-3.84	99.35	94.53	91 ± 6[a] 91 ± 4[c]
EuS	49.58	43.52	0.36	-4.95	4.44	92.42	87.90	86 ± 6[a] 86 ± 4[b]
EuSe	42.89	38.19	1.38	-2.54	2.77	82.32	76.50	66 ± 6[a] 72 ± 4[c]
Category III								
TbS	-29.85	155.87	-0.63	8.78	-0.71	132.87	122.00	-
TbSe	-35.14	144.32	-24.54	11.07	-2.86	92.47	106.10	-
ErS	-67.29	130.88	-0.92	27.66	0.17	89.94	98.20	99 ± 4[b]
ErSe	-183.70	9.72	32.65	41.80	-1.06	-100.92	82.70	-

[a]Ref 13 [b]Ref 30 [c] Ref 31

Table V. Dissociation energies at CBS in kcal mol^{-1}, with CCSD(T), paired with double-, triple- and quadruple-ξ basis sets and two different geometries.

	Geometry	**CBS**[a]	**CBS**[b]	**Exp.**[38]	**Exp.** [30]
TbS	CCSD(T)-DKH3	137.0	126.8	122.0	-
	PW91-DKH3	136.6	126.4		
TbSe	CCSD(T)-DKH3	124.7	110.7	106.1	-
	PW91-DKH3	124.6	110.6		
ErS	CCSD(T)-DKH3	92.5	81.7	98.2	99 ± 4
	PW91-DKH3	91.5	80.7		
ErSe	CCSD(T)-DKH3	-125.8	-2.2	82.7	-
	PW91-DKH3	-129.8	no convergence		

[a] Using restricted Hartree-Fock as an initial guess for the orbitals

[b] Using restricted PW91 as an initial guess for the orbitals

Table VI. Erbium selenide dissociation energies (kcal mol^{-1}) using CCSD(T)-DKH3 geometries, paired with double-, triple- and quadruple-ξ basis sets, considering four families of DFT functionals, ZPVE (CCSD(T)/DKH3 geometry) and spin-orbit corrected.

DFT functional	Double-ξ	Triple-ξ	Quadruple-ξ	Exp.[38]
TPSS	245.3	252.5	193.3	82.7
B3LYP	86.3	92.0	70.8	
M06-L	134.5	126.4	81.0	
PW91	234.0	217.2	209.2	

Table VII. CI vectors from CASSCF calculations for the equilibrium bond lengths of sulfide and selenide complexes. 0, α, 2 and "-" correspond to orbital occupations: zero, one (α-spin), two (doubly occupied), and not included in the active space electrons, respectively.

Molecules	Coeff.	$4f_{yz^2}$	$4f_{xyz}$	$4f_{y(3x^2-y^2)}$	$4f_{xz^2}$	$4f_{z(x^2-y^2)}$	$4f_{x(x^2-3y^2)}$	$4f_{z^3}$	6_s	n[a] px	n[a] p_y	n[a] p_z	$5d_{zy}$	$5d_{xy}$	$5d_{yx}$	$5d_{x^2-y^2}$	$5d_{z^2}$
PrS (^{4}H)	0.71	0	0	0	0	α	α	0	α	2	2	2	-	-	-	-	-
	-0.71	0	α	α	0	0	0	0	α	2	2	2	-	-	-	-	-
NdS (^{5}I)	0.50	α	α	α	0	0	0	0	α	2	2	2	-	-	-	-	-
	-0.50	0	α	0	α	0	α	0	α	2	2	2	-	-	-	-	-
	0.50	0	0	0	α	α	α	0	α	2	2	2	-	-	-	-	-
	-0.50	0	0	α	α	α	0	0	α	2	2	2	-	-	-	-	-
SmS ($^7\Delta$)	0.87	0	α	α	0	α	α	α	α	2	2	2	-	-	-	-	-
	0.49	α	0	α	α	0	α	α	α	2	2	2	-	-	-	-	-
GdS ($^9\Sigma^-$)	0.99	α	α	α	α	α	α	α	α	2	2	2	0	0	0	0	0
EuS ($^8\Sigma^-$)	0.99	α	α	α	α	α	α	0	α	2	2	2		-	-	-	-
TbS ($^8\Phi$)	1.0	α	α	α	α	2	α	α	α	2	2	2	-	-	-	-	-
ErS ($^5\Delta$)	0.55	2	2	2	α	2	α	α	α	2	2	2	-	-	-	-	-
	-0.34	α	2	2	2	α	α	2	α	2	2	2	-	-	-	-	-
	-0.34	α	2	α	α	2	2	2	α	2	2	2	-	-	-	-	-
	-0.32	2	α	2	2	α	α	2	α	2	2	2	-	-	-	-	-
	0.32	2	α	α	α	2	2	2	α	2	2	2	-	-	-	-	-
	-0.32	2	2	2	α	α	2	α	α	2	2	2	-	-	-	-	-
	0.32	2	2	α	2	2	α	α	α	2	2	2	-	-	-	-	-
LuS ($^2\Sigma^+$)	-0.96	2	2	2	2	2	2	2	α	2	2	2	0	0	0	0	0
PrSe (^{4}H)	0.71	0	0	α	0	α	0	0	α	2	2	2	-	-	-	-	-
	0.71	0	0	0	0	α	α	0	α	2	2	2	-	-	-	-	-
NdSe (^{5}I)	0.50	α	α	α	0	0	0	0	α	2	2	2	-	-	-	-	-
	-0.50	0	α	0	α	0	α	0	α	2	2	2	-	-	-	-	-
	0.50	0	0	α	α	α	0	0	α	2	2	2	-	-	-	-	-
	-0.50	α	0	0	0	α	α	0	α	2	2	2	-	-	-	-	-
SmSe ($^7\Delta$)	0.86	0	α	α	0	α	α	α	α	2	2	2	-	-	-	-	-
	0.50	α	0	α	α	0	α	α	α	2	2	2	-	-	-	-	-
EuSe ($^8\Sigma^-$)	0.99	α	α	α	α	α	α	0	α	2	2	2	-	-	-	-	-
GdSe ($^9\Sigma^-$)	1.00	α	α	α	α	α	α	α	α	2	2	2	0	0	0	0	0
TbSe ($^8\Phi$)	1.00	α	α	α	α	2	α	α	α	2	2	2	-	-	-	-	-
ErSe ($^5\Delta$)	0.55	2	2	2	α	2	α	α	α	2	2	2	-	-	-	-	-
	-0.34	α	2	2	2	α	α	2	α	2	2	2	-	-	-	-	-
	-0.34	α	2	α	α	2	2	2	α	2	2	2	-	-	-	-	-
	-0.32	2	α	2	2	α	α	2	α	2	2	2	-	-	-	-	-
	0.32	2	α	α	α	2	2	2	α	2	2	2	-	-	-	-	-
	-0.32	2	2	2	α	α	2	α	α	2	2	2	-	-	-	-	-
	0.32	2	2	α	2	2	α	α	α	2	2	2	-	-	-	-	-
LuSe ($^2\Sigma^+$)	0.94	2	2	2	2	2	2	2	α	2	2	2	0	0	0	0	0

[a] correspond to 3p for sulfur and 4p for selenium

Table VIII. Multireference considerations for lanthanide sulfides and selenides using CCSD(T)/DKH3 geometries. T_1 and D_1 are common diagnostics, $|T_{1max}|$ and $|T_{2max}|$ are the absolute values of the largest amplitudes, and S^2 is the spin contamination.

	T_1	D_1	$\|T_{1max}\|$	$\|T_{2max}\|$	Spin contamination (S^2)
PrS	0.03	0.11	0.12	0.20	0.004
NdS	0.03	0.10	0.13	0.11	0.003
SmS	0.03	0.09	0.07	-	0.01
EuS	0.03	0.03	0.08	-	0.003
GdS	0.03	0.10	0.12	-	0.03
TbS	0.03	0.10	0.13	-	0.007
ErS	0.03	0.10	0.13	0.06	0.002
LuS	0.03	0.10	0.13	-	0.001
PrSe	0.04	0.11	0.13	0.20	0.005
NdSe	0.04	0.11	0.13	0.11	0.004
SmSe	0.03	0.10	0.08	-	0.01
EuSe	0.03	0.11	0.09	-	0.003
GdSe	0.03	0.10	0.13	-	0.05
TbSe	0.03	0.10	0.13	-	0.009
ErSe	0.05	0.18	0.25	0.10	0.009
LuSe	0.03	0.11	0.15	-	0.001

IV. Conclusion

In this work, bond dissociation energy predictions of lanthanide sulfides and selenides were investigated. Three different methods were considered for geometry optimizations. While DFT offers a fast solution for geometry optimizations, CCSD(T) is a more reliable methodology for lanthanide sulfide and selenide diatomics. Between one- and two-component Hamiltonian CCSD(T) calculations, the difference in the optimized geometry was small. A one component Hamiltonian with ECP basis set offers a balance between speed and reliability that can be used in the future.

f-ccCA is shown here to be a reliable composite scheme. For bond dissociation energy predictions, eight (Pr, Sm, Gd and Lu complexed with S and Se) of the complexes had energies within 2 kcal mol^{-1} from the experimental BDEs.It does have some limitations for molecules with significant multireference character. However, herein some different routes are offered, which can be helpful in addressing these limitations. A Breit-Pauli Hamiltonian for spin-orbit calculations proved to be paramount to analyze ground state contributions, orbital occupations, identify state symmetries, and predict accurate spin-orbit contributions while having a mixture of ground and several excited states. Multireference diagnostics aid in identifying problematic molecules and help explain differences from experimental values. Four complexes (EuS, NdS, EuSe and NdSe) had BDEs were within 6 kcal mol^{-1} from experiment. Some of these complexes have large multireference character, or different RHF/CCSD(T) electronic configurations for the ground state when compared to those arising from CAS/MRCI, which led to deviations from experiment. For TbS and TbSe, DFT (PW91) provided better quality orbitals than CCSD(T), for the description of their ground state. The degree of multireference character observed for ErS and ErSe was not easily overcome with single reference methods. The use of DFT orbitals in CCSD(T) was not a suitable route for these complexes and even considering different functionals for energy dissociation predictions led to fortuitus results. Even though, M06-L at a quadruple-ζ level is only 1.7 kcal mol^{-1} from experiment, for ErSe this result should be treated with caution based on the inconsistent behavior of DFT for the dissociation energies of transition metal and lanthanide containing molecules,[25] as well as the significant and inconsistent shifts in energy with respect to increasing basis set level.

The complexity of these calculations is tremendous, and the aim of this project was to address gaps in the literature in terms of the lanthanide chemistry of sulfides and selenides. For EuS, SmS, EuSe and SmSe at CAS/MRCI a new $4f^x6s^1$ (x=number of electrons) electronic configuration of the lanthanide was postulated for the ground state of these complexes. Overall, this study offers routes that are important in calculating accurate bond dissociation energies for small lanthanide species without significant multireference wavefunction character, though great care is needed to properly describe the correct ground states.

Supplementary Material

The data that support the findings of this study are avail- able within the article and its supplementary material and from the corresponding author upon reasonable request. It is composed of the *f*-ccCA steps for each molecules using both the PW91-DK3 and CCSD(T)/ECP geometries as well a the corresponding multireference diagnostic.

Acknowledgments

This material is based upon work supported by the National Science Foundation under Grant No. CHE-1900086. This work utilized computational facilities at the Institute for Cyber-Enabled Research (ICER) at Michigan State University. The authors acknowledge the tremendous impact and contributions of Professor Klaus Ruedenberg in the field of Chemistry.

References:

[1] J.-C.G. Bünzli, Trends Chem. **1**, 751 (2019).
[2] D. Freedman, S. Sayan, T.J. Emge, M. Croft, and J.G. Brennan, J. Am. Chem. Soc. **121**, 11713 (1999).
[3] D. Freedman, T.J. Emge, and J.G. Brennan, Inorg. Chem. **38**, 4400 (1999).
[4] J.H. Melman, M. Fitzgerald, D. Freedman, T.J. Emge, and J.G. Brennan, J. Am. Chem. Soc. **121**, 10247 (1999).
[5] Y.G. Choi, K.H. Kim, S.H. Park, and H. Jong, J. Appl. Phys. **88**, 3832 (2000).
[6] Y.B. Shin, J. Heo, and S. Kim, *Modification of the Local Phonon Modes and Electron-Phonon Coupling Strengths in Dy 3q-Doped Sulfide Glasses for Efficient 1.3 Mm Amplification* (2000).
[7] Y. Luo, X. Wan, Y. Ito, S. Takami, M. Kubo, and A. Miyamoto, Chem. Phys. **282**, 197 (2002).
[8] S. Sujecki, Fibers **6**, 25 (2018).
[9] R.W. Crane, Ł. Sójka, D. Furniss, J. Nunes, E. Barney, M.C. Farries, T.M. Benson, S. Sujecki, and A.B. Seddon, Opt. Express **28**, 12373 (2020).
[10] A. V Golubkov, M.M. Kazanin, V. V Kaminskii, V. V Sokolov, S.M. Solov'ev, and L.N. Trushnikova, Inorg. Mater. **39**, 1251 (2003).
[11] D.L. Chess, C.A. Chess, J. V. Biggers, and W.B. White, J. Am. Ceram. Soc. **66**, 18 (1983).
[12] S.B. Jundale and C.D. Lokhande, *Solar Energy Materials and Solar Ceils (Photo) Electrochemical Studies on p-Sm 2 S 3 Films* (1992).
[13] M.S. Chandrasekharaiah and K.A. Gingerich, in (Elsevier, 1989), pp. 409–431.

[14] E. Murad and D.L. Hildenbrand, J. Chem. Phys. **73**, 4005 (1980).
[15] K.A. Gingerich, J. Chem. Phys. **50**, 2255 (1969).
[16] A. Ciccioli, G. Gigli, G. Meloni, and E. Testani, J. Chem. Phys. **127**, 054303 (2007).
[17] M. Dolg, W. Liu, and S. Kalvoda, Int. J. Quantum Chem. **76**, 359 (2000).
[18] J.P. Perdew, Phys. Rev. B **33**, 8822 (1986).
[19] J.P. Perdew and Y. Wang, Phys. Rev. B **45**, 13244 (1992).
[20] J.P. Perdew and Y. Wang, Phys. Rev. B **98**, 079904 (2018).
[21] C. Lee, W. Yang, and R.G. Parr, Phys. Rev. B **37**, 785 (1988).
[22] W. Xu, W.-X. Ji, and S.-G. Wang, Comput. Theor. Chem. **1068**, 81 (2015).
[23] V.G. Solomonik and A.N. Smirnov, J. Chem. Theory Comput. **13**, 5240 (2017).
[24] S. Grimmel, G. Schoendorff, and A.K. Wilson, J. Chem. Theory Comput. **12**, 1259 (2016).
[25] L.E. Aebersold, S.H. Yuwono, G. Schoendorff, and A.K. Wilson, J. Chem. Theory Comput. **13**, 2831 (2017).
[26] L.E. Aebersold and A.K. Wilson, J. Phys. Chem. A **125**, 7029 (2021).
[27] A.J. Cohen, P. Mori-Sánchez, and W. Yang, Science (80-.). **321**, 792 (2008).
[28] O. Adeyiga, O. Suleiman, N.K. Dandu, and S.O. Odoh, J. Chem. Phys. **151**, 134102 (2019).
[29] P. Coppens, S. Smoes, and J. Drowart, Trans. Faraday Soc. **63**, 2140 (1967).
[30] S. Smoes, P. Coppens, C. Bergman, and J. Drowart, Trans. Faraday Soc. **65**, 682 (1969).
[31] C. Bergman, P. Coppens, J. Drowart, and S. Smoes, Trans. Faraday Soc. **66**, 800 (1970).
[32] S. Nagai, K. Niwa, M. Shinmei, and T. Yokokawa, *Heats If Atomization, Dissociation Energies and Heats of Sublimation of Several Rare Earth Monochalcogenides* (Pergamon Press, 1973).
[33] M.S. Oakley, L. Gagliardi, and D.G. Truhlar, Molecules **26**, 2881 (2021).
[34] M.D. Morse, Acc. Chem. Res. **52**, 119 (2019).
[35] A. Sevy, J.J. Sorensen, T.D. Persinger, J.A. Franchina, E.L. Johnson, and M.D. Morse, J. Chem. Phys. **147**, 084301 (2017).
[36] A. Sevy, E. Tieu, and M.D. Morse, J. Chem. Phys. **149**, 174307 (2018).
[37] A. Sevy, D.M. Merriles, R.S. Wentz, and M.D. Morse, J. Chem. Phys. **151**, 024302 (2019).
[38] J.J. Sorensen, E. Tieu, and M.D. Morse, J. Chem. Phys. **154**, 124307 (2021).
[39] J.A. Pople, M. Head-Gordon, D.J. Fox, K. Raghavachari, and L.A. Curtiss, J. Chem. Phys. **90**, 5622 (1989).
[40] L.A. Curtiss, C. Jones, G.W. Trucks, K. Raghavachari, and J.A. Pople, J. Chem. Phys. **93**, 2537 (1990).
[41] L.A. Curtiss, K. Raghavachari, G.W. Trucks, and J.A. Pople, J. Chem. Phys. **94**, 7221 (1991).
[42] L.A. Curtiss, K. Raghavach Ari, P.C. Redfern, V. Rassolov, and J.A. Pople, J. Chem. Phys. **109**, 7764 (1998).
[43] L.A. Curtiss, P.C. Redfern, K. Raghavachari, and J.A. Pople, J. Chem. Phys. **114**, 108 (2001).
[44] L.A. Curtiss, P.C. Redfern, and K. Raghavachari, J. Chem. Phys. **126**, 084108 (2007).
[45] J.M.L. Martin and G. De Oliveira, J. Chem. Phys. **111**, 1843 (1999).
[46] S. Parthiban and J.M.L. Martin, J. Chem. Phys. **114**, 6014 (2001).
[47] A. Daniel Boese, M. Oren, O. Atasoylu, J.M.L. Martin, M. Kállay, and J. Gauss, J. Chem. Phys. **120**, 4129 (2004).
[48] A. Karton, E. Rabinovich, J.M.L. Martin, and B. Ruscic, J. Chem. Phys. **125**, 144108 (2006).
[49] G.A. Petersson, A. Bennett, T.G. Tensfeldt, M.A. Al-Laham, W.A. Shirley, and J. Mantzaris, J. Chem. Phys. **89**, 2193 (1988).
[50] G.A. Petersson and M.A. Al-Laham, J. Chem. Phys. **94**, 6081 (1991).
[51] G.A. Petersson, T.G. Tensfeldt, and J.A. Montgomery, J. Chem. Phys. **94**, 6091 (1991).
[52] J.W. Ochterski, G.A. Petersson, and J.A. Montgomery, J. Chem. Phys. **104**, 2598 (1996).
[53] J.A. Montgomery, J.W. Ochterski, and G.A. Petersson, J. Chem. Phys. **101**, 5900 (1994).
[54] J.A. Montgomery, M.J. Frisch, J.W. Ochterski, and G.A. Petersson, J. Chem. Phys. **110**, 2822 (1999).
[55] A. Tajti, P.G. Szalay, A.G. Császár, M. Kállay, J. Gauss, E.F. Valeev, B.A. Flowers, J. Vázquez, and J.F. Stanton, J. Chem. Phys. **121**, 11599 (2004).
[56] Y.J. Bomble, J. Vázquez, M. Kállay, C. Michauk, P.G. Szalay, A.G. Császár, J. Gauss, and J.F.

Stanton, J. Chem. Phys. **125**, (2006).
[57] M.E. Harding, J. Vázquez, B. Ruscic, A.K. Wilson, J. Gauss, and J.F. Stanton, J. Chem. Phys. **128**, 114111 (2008).
[58] J.H. Thorpe, C.A. Lopez, T.L. Nguyen, J.H. Baraban, D.H. Bross, B. Ruscic, and J.F. Stanton, J. Chem. Phys. **150**, 224102 (2019).
[59] D. Feller, K.A. Peterson, and D.A. Dixon, J. Chem. Phys. **129**, 204105 (2008).
[60] K.A. Peterson, D. Feller, and D.A. Dixon, Theor. Chem. Acc. **131**, 1079 (2012).
[61] D.A. Dixon, D. Feller, and K.A. Peterson, in *Annu. Rep. Comput. Chem.*, edited by R.A.B.T.-A.R. in C.C. Wheeler (Elsevier, 2012), pp. 1–28.
[62] N.J. DeYonker, T.R. Cundari, and A.K. Wilson, J. Chem. Phys. **124**, 114104 (2006).
[63] N.J. DeYonker, T. Grimes, S. Yockel, A. Dinescu, B. Mintz, T.R. Cundari, and A.K. Wilson, J. Chem. Phys. **125**, 104111 (2006).
[64] N.J. DeYonker, D.S. Ho, A.K. Wilson, and T.R. Cundari, J. Phys. Chem. A **111**, 10776 (2007).
[65] N.J. DeYonker, B. Mintz, T.R. Cundari, and A.K. Wilson, J. Chem. Theory Comput. **4**, 328 (2008).
[66] N.J. DeYonker, K.A. Peterson, G. Steyl, A.K. Wilson, and T.R. Cundari, J. Phys. Chem. A **111**, 11269 (2007).
[67] N.J. DeYonker, T.G. Williams, A.E. Imel, T.R. Cundari, and A.K. Wilson, J. Chem. Phys. **131**, 024106 (2009).
[68] W. Jiang, N.J. Deyonker, J.J. Determan, and A.K. Wilson, J. Phys. Chem. A **116**, 870 (2012).
[69] B.K. Welch, N.M.S. Almeida, and A.K. Wilson, Mol. Phys. **119**, e1963001 (2021).
[70] A. Sevy, D.J. Matthew, and M.D. Morse, J. Chem. Phys. **149**, 44306 (2018).
[71] D.M. Merriles, A. Sevy, C. Nielson, and M.D. Morse, J. Chem. Phys. **153**, 24303 (2020).
[72] D.M. Merriles, K.H. Tomchak, J.C. Ewigleben, and M.D. Morse, J. Chem. Phys. **155**, 144303 (2021).
[73] B.K. Welch and A.K. Wilson, unpublished (n.d.).
[74] N.M.S. Almeida, R.G. McKinlay, and M.J. Paterson, Chem. Phys. **446**, 86 (2015).
[75] R.G. McKinlay, N.M.S. Almeida, J.P. Coe, and M.J. Paterson, J. Phys. Chem. A **119**, 10076 (2015).
[76] C. Edmiston and K. Ruedenberg, Rev. Mod. Phys. **35**, 457 (1963).
[77] K. Ruedenberg, J. Chem. Phys. **19**, 1459 (1951).
[78] K. Ruedenberg, Rev. Mod. Phys. **34**, 326 (1962).
[79] K. Ruedenberg, J. Phys. Chem. A **114**, 8490 (2010).
[80] J.P. Perdew, K. Burke, and Y. Wang, Phys. Rev. B **54**, 16533 (1996).
[81] Z. Fang, M. Vasiliu, K.A. Peterson, and D.A. Dixon, J. Chem. Theory Comput. **13**, 1057 (2017).
[82] R.G. McKinlay, N.M.S. Almeida, J.P. Coe, and M.J. Paterson, J. Phys. Chem. A **119**, 10076 (2015).
[83] G. Jansen and B.A. Hess, Phys. Rev. A **39**, 6016 (1989).
[84] Q. Lu and K.A. Peterson, J. Chem. Phys. **145**, 054111 (2016).
[85] A.K. Wilson, D.E. Woon, K.A. Peterson, and T.H. Dunning, J. Chem. Phys. **110**, 7667 (1999).
[86] W.A. de Jong, R.J. Harrison, and D.A. Dixon, J. Chem. Phys. **114**, 48 (2000).
[87] N.B. Balabanov and K.A. Peterson, J. Chem. Phys. **123**, 064107 (2005).
[88] M. Dolg, H. Stoll, and H. Preuss, J. Chem. Phys. **90**, 1730 (1989).
[89] X. Cao and M. Dolg, J. Chem. Phys. **115**, 7348 (2001).
[90] X. Cao, M. Dolg, and H. Stoll, J. Chem. Phys. **118**, 487 (2002).
[91] K.A. Peterson, D. Figgen, E. Goll, H. Stoll, and M. Dolg, J. Chem. Phys. **119**, 11113 (2003).
[92] N.M.S. Almeida, T.R.L. Melin, and A.K. Wilson, J. Chem. Phys. **154**, 244304 (2021).
[93] H.-J. Werner, P.J. Knowles, F.R. Manby, J.A. Black, K. Doll, A. Heßelmann, D. Kats, A. Köhn, T. Korona, D.A. Kreplin, Q. Ma, T.F. Miller, A. Mitrushchenkov, K.A. Peterson, I. Polyak, G. Rauhut, and M. Sibaev, J. Chem. Phys. **152**, 144107 (2020).
[94] T.G. Williams, N.J. DeYonker, and A.K. Wilson, J. Chem. Phys. **128**, 044101 (2008).
[95] A. Halkier, T. Helgaker, P. Jørgensen, W. Klopper, and J. Olsen, Chem. Phys. Lett. **302**, 437 (1999).
[96] K.A. Peterson, D.E. Woon, and T.H. Dunning, J. Chem. Phys. **100**, 7410 (1994).
[97] A. Kramida, Yu. Ralchenko, J. Reader, and NIST ASD Team, (2020).
[98] T.J. Lee and P.R. Taylor, Int. J. Quantum Chem. **36**, 199 (2009).

[99] T.J. Lee, J.E. Rice, G.E. Scuseria, and H.F. Schaefer, Theor. Chim. Acta **75**, 81 (1989).
[100] C.L. Janssen and I.M.B. Nielsen, Chem. Phys. Lett. **290**, 423 (1998).
[101] J. Tao, J.P. Perdew, V.N. Staroverov, and G.E. Scuseria, Phys. Rev. Lett. **91**, 146401 (2003).
[102] Y. Zhao and D.G. Truhlar, J. Chem. Phys. **125**, 194101 (2006).
[103] A.D. Becke, J. Chem. Phys. **98**, 1372 (1993).
[104] W. Jiang, N.J. Deyonker, and A.K. Wilson, J. Chem. Theory Comput. **8**, 460 (2012).
[105] E.R. Davidson, Annu. Rev. Phys. Chem. **70**, 1 (2019).
[106] G. Czack, H. Hein, I. Hinz, H. Bergmann, P. Kuhn, in 8th ed. (Springer-Verlag, New York, 1983).

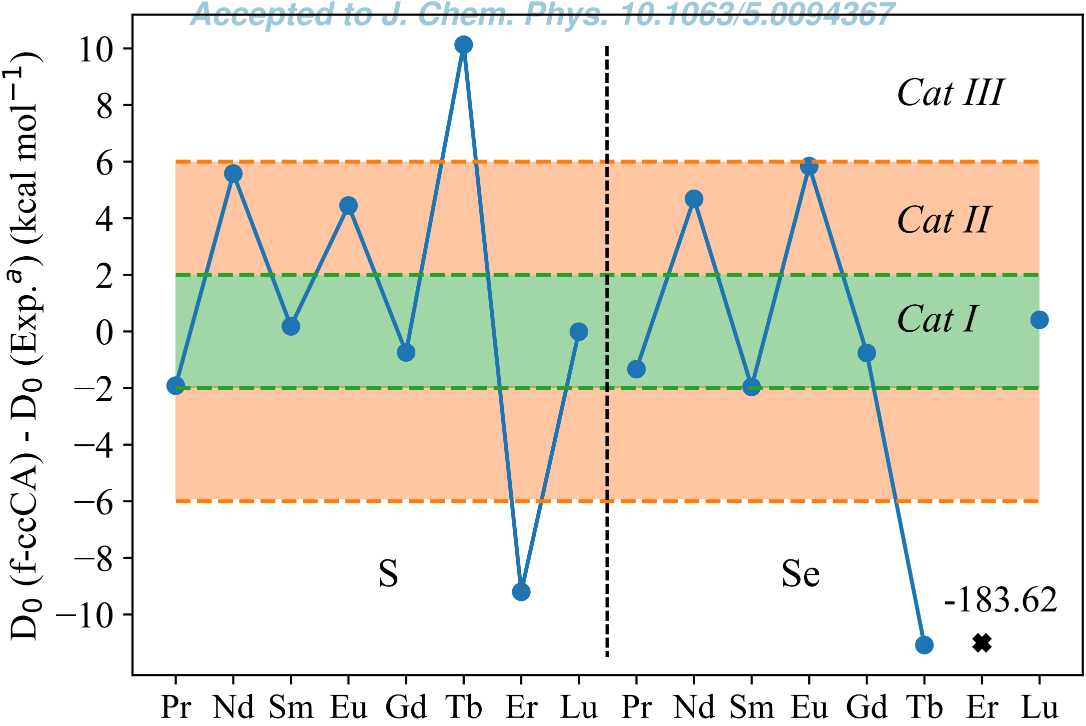
D$_0$ (f-ccCA) - D$_0$ (Exp.^{a}) (kcal mol^{-1})
10
8
6
4
2
0
−2
−4
−6
−8
−10
Cat III
Cat II
Cat I
S
Se
-183.62
Pr
Nd
Sm
Eu
Gd
Tb
Er
Lu
Pr
Nd
Sm
Eu
Gd
Tb
Er
Lu